

PDF hosted at the Radboud Repository of the Radboud University Nijmegen

The following full text is a preprint version which may differ from the publisher's version.

For additional information about this publication click this link.

<http://hdl.handle.net/2066/116988>

Please be advised that this information was generated on 2017-12-05 and may be subject to change.

A strong magnetic field around the supermassive black hole at the centre of the Galaxy

R. P. Eatough¹, H. Falcke^{2,3,1}, R. Karuppusamy¹, K. J. Lee¹, D. J. Champion¹, E. F. Keane⁴, G. Desvignes¹, D. H. F. M. Schnitzeler¹, L. G. Spitler¹, M. Kramer^{1,4}, B. Klein^{5,1}, C. Bassa⁴, G. C. Bower⁶, A. Brunthaler¹, I. Cognard^{7,8}, A. T. Deller³, P. B. Demorest⁹, P. C. C. Freire¹, A. Kraus¹, A. G. Lyne⁴, A. Noutsos¹, B. Stappers⁴ & N. Wex¹

¹*Max-Planck-Institut für Radioastronomie, Auf dem Hügel 69, D-53121 Bonn, Germany*

²*Department of Astrophysics, Institute for Mathematics, Astrophysics and Particle Physics, Radboud University, PO Box 9010, 6500 GL Nijmegen, The Netherlands*

³*ASTRON, P.O. Box 2, 7990 AA Dwingeloo, The Netherlands*

⁴*Jodrell Bank Centre for Astrophysics, School of Physics and Astronomy, The University of Manchester, Manchester, M13 9PL, UK*

⁵*University of Applied Sciences Bonn-Rhein-Sieg, Grantham-Allee 20, D-53757 Sankt Augustin, Germany*

⁶*UC Berkeley Astronomy Dept, B-20 Hearst Field Annex, Berkeley, CA 94720-3411*

⁷*LPC2E / CNRS - Université d'Orléans, 45071 Orléans, France*

⁸*Nançay/Paris Observatory, 18330 Nançay, France*

⁹*National Radio Astronomy Observatory, 520 Edgemont Road, Charlottesville, VA 22903, USA*

The centre of our Milky Way harbours the closest candidate for a supermassive black hole¹.

The source is thought to be powered by radiatively inefficient accretion of gas from its

environment². This form of accretion is a standard mode of energy supply for most galactic nuclei. X-ray measurements have already resolved a tenuous hot gas component from which it can be fed³. However, the magnetization of the gas, a crucial parameter determining the structure of the accretion flow, remains unknown. Strong magnetic fields can influence the dynamics of the accretion, remove angular momentum from the infalling gas⁴, expel matter through relativistic jets⁵ and lead to the observed synchrotron emission⁶⁻⁸. Here we report multi-frequency measurements with several radio telescopes of a newly discovered pulsar close to the Galactic Centre⁹⁻¹² and show that its unusually large Faraday rotation indicates a dynamically relevant magnetic field near the black hole. If this field is accreted down to the event horizon it provides enough magnetic flux to explain the observed emission from the black hole, from radio to X-rays.

Linearly polarized radio waves that pass through a magnetized medium experience Faraday rotation. The resulting rotation of the polarization vector is given by $\Delta\phi = \text{RM}\lambda^2$, where the rotation measure $\text{RM} = e^3/(2\pi m_e^2 c^4) \int B(s) n(s) ds$, which depends on the line-of-sight magnetic field B , the free electron density n , and the path length s . The radio emission associated with the Galactic Centre black hole, Sagittarius A* (Sgr A*), has $\text{RM} = -5 \times 10^5 \text{ rad m}^{-2}$, which is the highest known RM of any source in the Galaxy, and is believed to be due to a column of hot, magnetized gas from the accretion flow onto the black hole^{13,14}.

Sgr A* itself, however, only probes the innermost scales of accretion. For most models¹⁴ the term $B(r) n(r)$ decays faster than r^{-1} , where r is the radial distance from the black hole.

Consequently, the Faraday rotation is dominated by the smallest scales. To measure the magnetization of the accretion flow on the outermost scales other polarized radio sources, such as pulsars, are needed. A pulsar closely orbiting Sgr A* would also be an unparalleled tool for testing the space-time structure around the black hole¹⁵. Despite predictions that there are in excess of a thousand pulsars in the central parsec of the Galaxy,¹⁶ there has been a surprising lack of detections,¹⁷ potentially due to severe interstellar dispersion and scattering in the inner Galaxy¹⁸.

Recently the *Swift* telescope detected a bright X-ray flare⁹ near Sgr A* ($\sim 3'' = 0.12$ pc projected offset¹⁹ at a Galactic Centre distance $d = 8.3$ kpc). Subsequent X-ray observations by the *NuSTAR* telescope resulted in the detection of pulsations at a period of 3.76 s¹⁰. This behaviour is indicative of a magnetar, a highly magnetized pulsar, in outburst. During radio follow-up observations at the Effelsberg observatory on April 28th, a first weak detection of pulsations, with spin parameters matching those reported by *NuSTAR*, was made. Since then, the pulsar, PSR J1745–2900, has been consistently detected at Effelsberg, Nançay, the Karl G. Jansky Very Large Array (VLA), tentatively at Jodrell Bank (see Figure 1.) and elsewhere with the ATCA¹². Measurements of the delay in the arrival times of pulses at lower frequencies (2.5 GHz) with respect to higher frequency (8.35 GHz) yield an integrated column density of free electrons, the dispersion measure (DM), of 1778 ± 3 cm⁻³ pc – the highest value measured for any known pulsar. This is consistent with a source located within < 10 pc of the Galactic Centre, within the NE2001 density model of the Galaxy²⁰. Including this source, only four radio-emitting magnetars are known²¹ in the Milky Way, making a chance alignment unlikely. If we consider a uniform source distribution occupying a cylinder of radius 10 kpc and height 1 kpc, then the fraction of

sources present within an angular distance of $\sim 3''$ around Sgr A* is $\sim 3 \times 10^{-9}$. Given the current population of radio pulsars (~ 2000) and radio magnetars, the number present within the same region by chance will be $\sim 6 \times 10^{-6}$ and $\sim 1 \times 10^{-8}$ respectively.

The emission from the pulsar is highly linearly polarized^{12,22} (Figure 2.). Using the RM synthesis method²³ and measuring the Faraday rotation at three frequency bands and three different telescope sites, we derive a RM of $(-6.696 \pm 0.005) \times 10^4$ rad m⁻² (Figure. 3). This measurement is consistent with that presented elsewhere¹². The RM is the largest measured for any Galactic object other than Sgr A*^{13,14}, and is more than an order of magnitude larger than all the other RMs measured to within tens of parsecs from Sgr A*²⁴. The RM is also more than what can be optimistically expected as foreground²⁵. This constrains the Faraday screen to be within some ten parsecs from the Galactic Centre.

A frequently used estimate of the magnetic field is $B \geq \text{RM}/(0.81\text{DM})\mu\text{G}$, which gives $B \geq 50 \mu\text{G}$ ¹². However, this is not a stringent limit, since the DM and RM are dominated by very different scales. Hence, the extra information about the gas in the central ten parsecs must be used for a more robust magnetic field estimate.

There are two ionized gas phases in the Galactic Centre interstellar medium towards the line of sight of the pulsar which could be associated with the Faraday screen: a warm component from the Northern Arm of the gas streamer Sgr A West²⁶ that passes behind Sgr A* and a diffuse hot component seen in the X-rays³ with $T = 2.2 \times 10^7$ K. The warm gas in the Northern Arm has a width of > 0.1 pc, electron densities of $\sim 10^5$ cm⁻³ measured from radio recombination lines²⁶,

and a magnetic field of $\sim 2 \text{ mG}^{27}$. The inferred RM and DM for a source in or behind the Northern Arm are $\text{RM} \sim 2 \times 10^7 \text{ rad m}^{-2}$ for an ordered magnetic field and $\text{DM} \sim 10^4 \text{ pc cm}^{-3}$. The measured DM and RM values therefore place the pulsar and the screen *in front* of the Northern Arm²⁶.

Consequently, the Faraday screen must be associated with the hot gas component, for which no magnetic field estimates exist yet. The density in the hot gas shows a radial fall-off as a function of distance r from the black hole. At 0.4 pc ($10''$) one finds $n \sim 26 \text{ cm}^{-3}$, whereas at 0.06 pc ($1.5''$) one can infer $n \lesssim 160 \text{ cm}^{-3}$, using the optically thin thermal plasma model³. Further away at the 40 pc scale²⁸ ($17'$), the density has decreased to $0.1\text{--}0.5 \text{ cm}^{-3}$ and we can roughly describe the central parsecs with a density profile of the form $n(r) \simeq 26 \text{ cm}^{-3} (r/0.4 \text{ pc})^{-1}$. The contribution of this hot gas component to the DM is of order $10^2 \text{ cm}^{-3} \text{ pc}$. This is consistent with the modest increase of DM with respect to the hitherto closest pulsars to the Galactic Centre.

For a simple one-zone Faraday screen, where $\text{RM} \propto B(r) n(r) r$, we have $\text{RM} = 8.1 \times 10^5 (B(r)/\text{G})(n(r)/\text{cm}^{-3})(r/\text{pc}) \text{ rad m}^{-2}$. Using the density prescription above with a r^{-1} scaling, we find $B \gtrsim 8(\text{RM}/66960 \text{ m}^{-2})(n_0/26 \text{ cm}^{-3})^{-1} \text{ mG}$. This is a lower limit, since possible turbulent field components or field reversals reduce the RM. We note again that this RM is indeed dominated by the smallest distance scale, i.e., by the gas on scales of the de-projected distance, $r > 0.12 \text{ pc}$, of the pulsar from Sgr A*.

This value is higher than the magnetic field in the Northern Arm and also higher than the equipartition field in the hot phase at this scale. To bring thermal and magnetic energy into equipar-

tion, the gas density at $r \sim 0.12$ pc would need to increase by a factor of three to 260 cm^{-3} , yielding ~ 2.6 mG. Many field reversals within the Faraday screen would drive the magnetic field way beyond equipartition, suggesting that a relatively ordered magnetic field is pervading the hot gas close to the supermassive black hole.

As Sgr A* accretes from this magnetized hot phase, density and magnetic field will further increase inwards. Emission models of Sgr A* require about 30-100 G magnetic fields to explain the synchrotron radiation from near the event horizon⁶⁻⁸. Hence, if the gas falls from 3×10^5 Schwarzschild radii (0.12 pc) down to a few Schwarzschild radii, already a simple $B \propto r^{-1}$ scaling would be enough to provide several hundred Gauss magnetic fields. This is well within the range of most accretion models, where where equipartition between magnetic, kinetic, and gravitational energy in the accreting gas is assumed^{14,29}.

The field provided on the outer scale of the accretion flow onto Sgr A* is therefore sufficient to provide the necessary field on the small scales via simple accretion. Moreover, the availability of ordered magnetic fields would make the proposed formation of a jet-like outflow in Sgr A*³⁰ viable. Super-equipartition magnetic fields could also suppress accretion and help to explain the low accretion rate of Sgr A*.

At its projected separation PSR J1745–2900 could move (due to orbital motion) through the hot gas surrounding Sgr A* with several mas/yr and reveal RM variations as well as proper motion. Continued pulsar polarimetry and VLBI astrometry can readily measure these effects. Also, given that magnetars constitute only a small fraction of the pulsar population and the excess

DM towards the Galactic Centre is not too large, we expect additional observable radio pulsars to be lurking in the same region. Such pulsars could be used to map out the accretion region around the black hole in more detail, and even test its spacetime properties.

1. Genzel, R., Eisenhauer, F. & Gillessen, S. The Galactic Center massive black hole and nuclear star cluster. *Reviews of Modern Physics* **82**, 3121–3195 (2010).
2. Narayan, R. & Yi, I. Advection-dominated accretion: A self-similar solution. *Astrophys. J.* **428**, L13–L16 (1994).
3. Baganoff, F. K. *et al.* Chandra X-Ray Spectroscopic Imaging of Sagittarius A* and the Central Parsec of the Galaxy. *Astrophys. J.* **591**, 891–915 (2003).
4. Balbus, S. A. & Hawley, J. F. A powerful local shear instability in weakly magnetized disks. I - Linear analysis. II - Nonlinear evolution. *Astrophys. J.* **376**, 214–233 (1991).
5. Beckwith, K., Hawley, J. F. & Krolik, J. H. The Influence of Magnetic Field Geometry on the Evolution of Black Hole Accretion Flows: Similar Disks, Drastically Different Jets. *Astrophys. J.* **678**, 1180–1199 (2008).
6. Falcke, H. & Markoff, S. The jet model for Sgr A*: Radio and X-ray spectrum. *Astron. & Astrophys.* **362**, 113–118 (2000).
7. Mościbrodzka, M., Gammie, C. F., Dolence, J. C., Shiokawa, H. & Leung, P. K. Radiative Models of SGR A* from GRMHD Simulations. *Astrophys. J.* **706**, 497–507 (2009).

8. Dexter, J., Agol, E., Fragile, P. C. & McKinney, J. C. The Submillimeter Bump in Sgr A* from Relativistic MHD Simulations. *Astrophys. J.* **717**, 1092–1104 (2010). 1005.4062.
9. Kennea, J. A. *et al.* Swift Discovery of a New Soft Gamma Repeater, SGR J1745–29, near Sagittarius A*. *Astrophys. J.* **770**, L24 (2013).
10. Mori, K. *et al.* NuSTAR Discovery of a 3.76 s Transient Magnetar Near Sagittarius A*. *Astrophys. J.* **770**, L23 (2013).
11. Eatough, R. P. *et al.* Detection of radio pulsations from the direction of the NuSTAR 3.76 second X-ray pulsar at 8.35 GHz. *The Astronomer's Telegram* **5040**, 1 (2013).
12. Shannon, R. M. & Johnston, S. Radio properties of the magnetar near Sagittarius A* from observations with the Australia Telescope Compact Array. *ArXiv e-prints* (2013). 1305.3036.
13. Bower, G. C., Falcke, H., Wright, M. C. & Backer, D. C. Variable Linear Polarization from Sagittarius A*: Evidence of a Hot Turbulent Accretion Flow. *Astrophys. J.* **618**, L29–L32 (2005).
14. Marrone, D. P., Moran, J. M., Zhao, J.-H. & Rao, R. An Unambiguous Detection of Faraday Rotation in Sagittarius A*. *Astrophys. J.* **654**, L57–L60 (2007).
15. Liu, K., Wex, N., Kramer, M., Cordes, J. M. & Lazio, T. J. W. Prospects for Probing the Spacetime of Sgr A* with Pulsars. *Astrophys. J.* **747**, 1 (2012).
16. Wharton, R. S., Chatterjee, S., Cordes, J. M., Deneva, J. S. & Lazio, T. J. W. Multiwavelength Constraints on Pulsar Populations in the Galactic Center. *Astrophys. J.* **753**, 108 (2012).

17. Eatough, R. P. *et al.* Can we see pulsars around Sgr A*? The latest searches with the Effelsberg telescope. In *IAU Symposium*, vol. 291 of *IAU Symposium*, 382–384 (2013).
18. Lazio, T. J. W. & Cordes, J. M. Hyperstrong radio-wave scattering in the galactic center. ii. a likelihood analysis of free electrons in the galactic center. *Astrophys. J.* **505**, 715–731 (1998).
19. Rea, N. *et al.* Chandra localization of the soft gamma repeater in the Galactic Center region. *The Astronomer's Telegram* **5032**, 1 (2013).
20. Cordes, J. M. & Lazio, T. J. W. NE2001.I. A New Model for the Galactic Distribution of Free Electrons and its Fluctuations. *ArXiv Astrophysics e-prints* (2002). Preprint at <http://arxiv.org/abs/astroph/0207156>.
21. Lazarus, P., Kaspi, V. M., Champion, D. J., Hessels, J. W. T. & Dib, R. Constraining Radio Emission from Magnetars. *Astrophys. J.* **744**, 97 (2012).
22. Lee, K. J. *et al.* Polarisation profiles and rotation measure of PSR J1745-2900 measured at Effelsberg. *The Astronomer's Telegram* **5064**, 1 (2013).
23. Brentjens, M. A. & de Bruyn, A. G. Faraday rotation measure synthesis. *Astron. & Astrophys.* **441**, 1217–1228 (2005).
24. Law, C. J., Brentjens, M. A. & Novak, G. A Constraint on the Organization of the Galactic Center Magnetic Field Using Faraday Rotation. *Astrophys. J.* **731**, 36 (2011).

25. Bower, G. C., Backer, D. C., Zhao, J.-H., Goss, M. & Falcke, H. The Linear Polarization of Sagittarius A*. I. VLA Spectropolarimetry at 4.8 and 8.4 GHz. *Astrophys. J.* **521**, 582–586 (1999).
26. Zhao, J.-H. *et al.* The High-density Ionized Gas in the Central Parsec of the Galaxy. *Astrophys. J.* **723**, 1097–1109 (2010).
27. Plante, R. L., Lo, K. Y. & Crutcher, R. M. The magnetic fields in the galactic center: Detection of H1 Zeeman splitting. *Astrophys. J.* **445**, L113–L116 (1995).
28. Muno, M. P. *et al.* Diffuse X-Ray Emission in a Deep Chandra Image of the Galactic Center. *Astrophys. J.* **613**, 326–342 (2004).
29. Macquart, J.-P., Bower, G. C., Wright, M. C. H., Backer, D. C. & Falcke, H. The Rotation Measure and 3.5 Millimeter Polarization of Sagittarius A*. *Astrophys. J.* **646**, L111–L114 (2006).
30. Falcke, H., Mannheim, K. & Biermann, P. L. The galactic center radio jet. *Astron. & Astrophys.* **278**, L1–L4 (1993).

Acknowledgements The authors wish to thank D. D. Xu., P. Lazarus and L. Guillemot for useful discussions. We also thank O. Wucknitz and R. Beck for manuscript reading. R.K., L.G.S. and P.C.C.F. gratefully acknowledge the financial support by the European Research Council for the ERC Starting Grant BEACON under contract no. 279702. K.J.L. was funded by ERC Advanced Grant LEAP under contract no. 227947. H.F. acknowledges funding from an Advanced Grant of the European Research Council under the

European Unions Seventh Framework Programme (FP/2007-2013) / ERC Grant Agreement no. 227610.

This work was based on observations with the 100-m telescope of the MPIfR (Max-Planck-Institut für Radioastronomie) at Effelsberg. The Nanay radio telescope is part of the Paris Observatory, associated with the Centre National de la Recherche Scientifique (CNRS), and partially supported by the Région Centre in France. The National Radio Astronomy Observatory (NRAO) is a facility of the National Science Foundation operated under cooperative agreement by Associated Universities, Inc.

Correspondence Correspondence and requests for materials should be addressed to Ralph Eatough (email: reatough@mpifr-bonn.mpg.de).

Author contributions:

R. P. Eatough - Initial detections, observations performed with Effelsberg, and data processing.

H. Falcke - Observational and theoretical background, paper formulation.

R. Karuppusamy - Observational technical assistance and pulsar timing.

K. J. Lee - Polarization and RM measurements.

D. J. Champion - Pulsar timing solution.

E. F. Keane - Flux density calculations, observational assistance and observations at Jodrell Bank.

G. Desvignes - Observations Nançay.

D. H. F. M. Schnitzeler - Observational background, RM interpretation.

L. G. Spitler - Observational background, data processing and analysis.

M. Kramer - Observational background, RM interpretation.

B. Klein - technical observational assistance Effelsberg.

C. Bassa - Observations Jodrell Bank.

G. C. Bower - Observations VLA, RM interpretation.

A. Brunthaler - Observations VLA.

I. Cognard - Observations Nançay

A. T. Deller - Observations VLA

P. B. Demorest - Observations VLA

P. C. C. Freire - Observational background, pulsar timing.

A. Kraus - technical observational assistance Effelsberg.

A. G. Lyne - Observations Jodrell Bank, help with initial detections.

A. Noutsos - Observational background, RM interpretation.

B. Stappers - Observations Jodrell Bank.

N. Wex - Theoretical background, orbital characteristics.

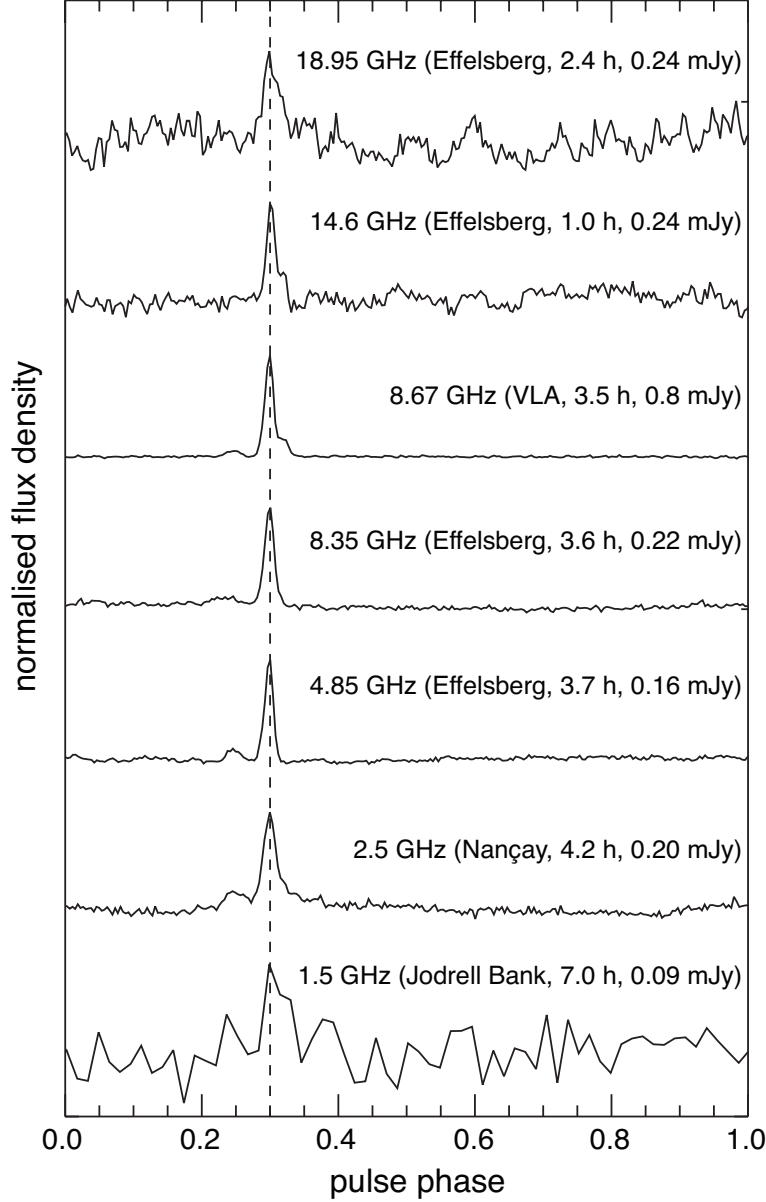


Figure 1: Average pulse profiles of PSR J1745-2900 at each of the radio frequencies where detections have been made. All observations have been centered on the X-ray position measured with *Chandra*¹⁹. The telescope used, the total observation time required to generate the profile, and the average flux density is indicated in brackets after the frequency label. In each case the profiles have been down-sampled from the original sampling interval to 256 phase bins (64 for the Jodrell data), and the peak flux density normalised to unity. The profiles have been aligned by the peak of the main pulse detected. By measuring accurate arrival times of the pulses, we have constructed a coherent timing solution; a model which tracks every single rotation of the pulsar. Over the period MJD 56414–56426, this model has given measurements of the spin period $P = 3.76354676(2)^{13}$ s and period derivative (spin-down) $\dot{P} = 6.82(3) \times 10^{-12}$; uncertainties on the last digit, given in brackets, are derived from the one-sigma error of timing model fit. Absolute timing from 1.5 to 8.35 GHz, has established that the main pulse in each profile is indeed aligned at each frequency.

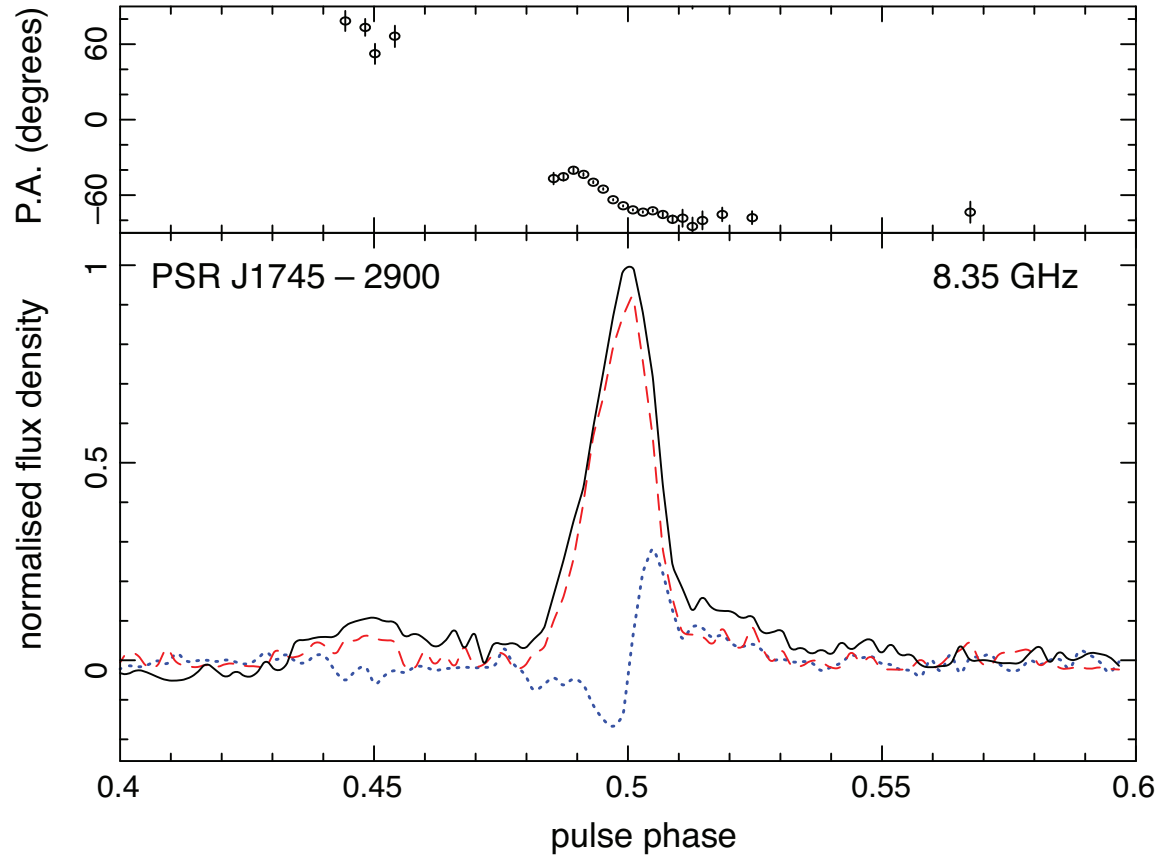


Figure 2: Pulse profile of PSR J1745-2900 at 8.35 GHz. After correcting for the Faraday rotation of $(-6.696 \pm 0.005) \times 10^4 \text{ rad m}^{-2}$, we can measure the intrinsic polarization across the pulse profile, together with the polarization position angle (PA). The degree of linear polarization (red dashed line) is nearly 100%, and a significant amount ($\sim 15\%$) of circular polarization (blue dotted line) is also detected. A consistent ‘S’-shape PA swing is measured at each frequency.

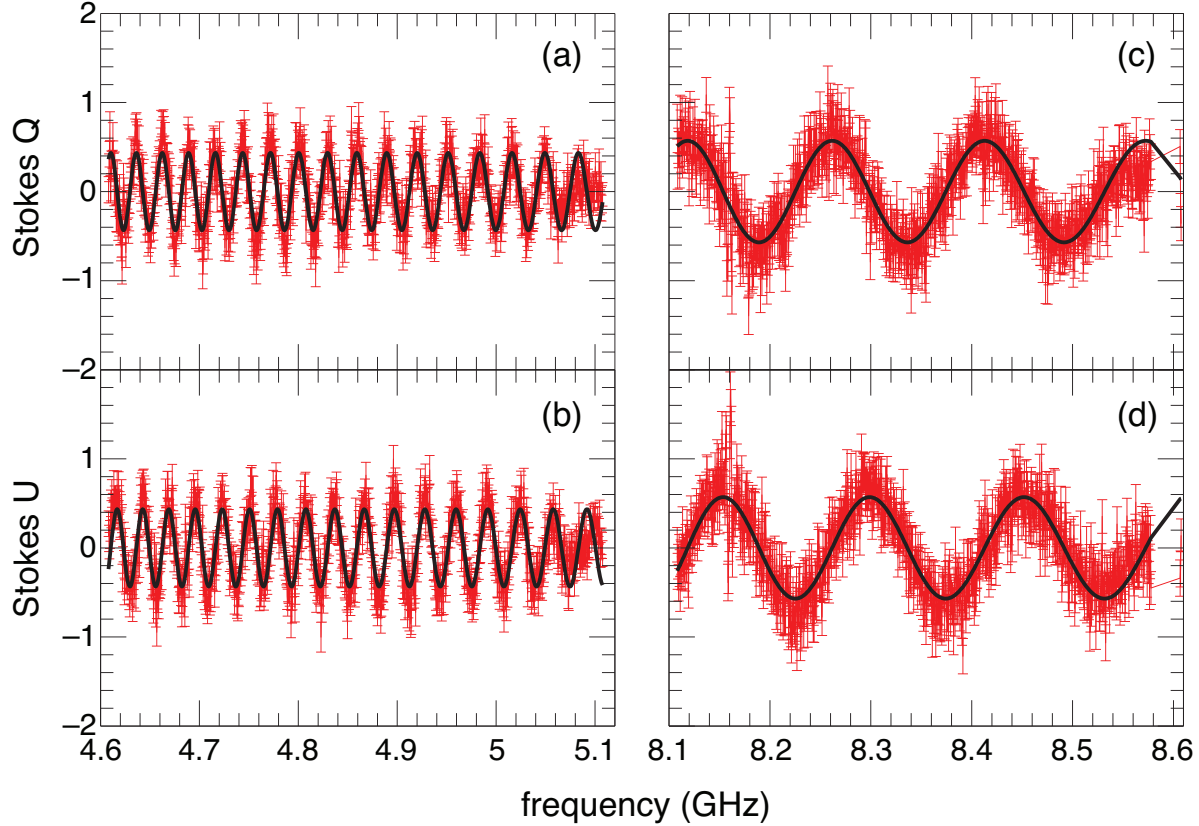


Figure 3: Rotation Measure (RM) synthesis analysis for the radio polarization of PSR J1745–2900. The red points, with one-sigma error bars given by the off-pulse baseline r.m.s of the polarization profile, present the observed polarized flux density in the Stokes parameters Q and U. Note polarization measurements were not possible at all frequencies due to hardware limitations. The RM is measured by a two-step method. Firstly, we perform the Fourier transformation of the polarization intensity to get the RM Faraday spectrum, of which the peak is used to find a rough estimation of the RM. Using such initial values, we then perform a least-squares fit to the Q and U curves to get the RM and its error. The black curves in this figure are the model values based on the best fit RM. The sinusoidal variation of Q and U due to Faraday rotation is clearly seen across the frequency bands centred at 4.85 (panels a. and b.) and 8.35 GHz (panels c. and d.). At 2.5 GHz the variation is so severe this signature is better seen in the RM spectrum not shown here. RM values derived at each frequency band are independently consistent: At 2.5 GHz $RM = (-6.70 \pm 0.01) \times 10^4 \text{ rad m}^{-2}$, at 4.85 GHz $RM = (-6.694 \pm 0.006) \times 10^4 \text{ rad m}^{-2}$ and at 8.35 GHz $RM = (-6.68 \pm 0.04) \times 10^4 \text{ rad m}^{-2}$. The RM has also been measured with the VLA at 8.67 GHz giving $(-6.70 \pm 0.04) \times 10^4 \text{ rad m}^{-2}$. The combined and appropriately weighted average is $(-6.696 \pm 0.005) \times 10^4 \text{ rad m}^{-2}$.